The leading mode of Indian Summer Monsoon precipitation variability during the last millennium

Ashish Sinha,[1] Max Berkelhammer,[2] Lowell Stott,[3] Manfred Mudelsee,[4,5] Hai Cheng,[6,7] and Jayant Biswas[8]

Received 4 May 2011; revised 21 June 2011; accepted 24 June 2011; published 4 August 2011.

[1] The "internally" generated intraseasonal variability of the Indian Summer Monsoon is characterized by intermittent periods of enhanced ("active") and deficient ("break") precipitation, which produce a quasi east-west precipitation dipole over the Indian subcontinent. Here we present multi-centennial-length and near annually-resolved reconstructions of monsoon precipitation, inferred from absolute-dated and instrumentally calibrated speleothem oxygen isotope records from regions (central and northeast India) that have diametric responses to active-break monsoon circulation patterns. On centennial timescales (AD 1400–2008), precipitation variability from these two regions exhibit opposing behavior, oscillating between periods with a persistently "active-dominated" (AD ~1700 to 2007) and a "break-dominated" (AD 1400 to ~1700) regime. The switch between these regimes occurs abruptly (within decades) at a time (AD ~ 1650–1700) when a proxy record of upwelling intensity from the Arabian Sea suggest an abrupt increase in the monsoon winds. On the basis of these observations, we hypothesize that the frequency distribution of active-break periods varies on centennial timescales, implying a leading role of internal dynamics in governing the ISM response to slowly-evolving changes in the external boundary conditions.
Citation: Sinha, A., M. Berkelhammer, L. Stott, M. Mudelsee, H. Cheng, and J. Biswas (2011), The leading mode of Indian Summer Monsoon precipitation variability during the last millennium, *Geophys. Res. Lett.*, *38*, L15703, doi:10.1029/2011GL047713.

1. Introduction

[2] The year-to-year variability in the Indian Summer Monsoon (ISM) seasonal mean precipitation is widely considered to arise from the slowly evolving external boundary conditions such as variations in Indo-Pacific tropical sea surface temperature (SST), snow-cover anomalies, and soil moisture [*Charney and Shukla*, 1981; *Webster et al.*, 1998]. In addition, a substantial component of variability also stems from chaotic intraseasonal oscillations in monsoon precipitation, referred to as active-break (A-B) spells, which exhibit a hierarchy of quasi-periods (3–7 days, 10–20 days and 30–60 days) [*Webster et al.*, 1998; *Krishnamurthy and Shukla*, 2000; *Goswami and Ajaya Mohan*, 2001]. The latter mode, in particular, affects precipitation over the entire Indian subcontinent through its influence on the superposition of northward propagating oscillations in the synoptic-scale convective systems, which are generated over the equatorial Indian Ocean (EIO) [*Webster et al.*, 1998; *Annamalai and Slingo*, 2001].

[3] Whereas a number of studies clearly indicate that the probability distribution function (PDF) of A-B periods strongly influence the seasonal mean precipitation amount [*Goswami and Ajaya Mohan*, 2001; *Goswami et al.*, 2006; *Rajeevan et al.*, 2010], the mechanisms that influence the PDF of A-B periods remains unknown. *Palmer* [1994] hypothesized that while A-B periods are intrinsically chaotic, external boundary forcing predisposes the monsoon system into "preferred states" (i.e., states exhibiting higher frequency of either active or break periods). The robustness of this hypothesis has critical implications with respect to monsoon predictability on intra-seasonal to decadal timescales. For example, if the A-B periods are purely chaotic and cannot be predicted in advance with sufficient lead times, than the potential for monsoon predictability will remain low. On the other hand, if there are global-scale "forcing functions" such as low frequency changes in tropical Pacific SSTs [*Webster et al.*, 1998], which modify the PDF of A-B periods, than ISM predictability is within the realm of possibility, at least in a probabilistic, if not deterministic sense [*Webster et al.*, 1998; *Goswami et al.*, 2006].

[4] The ISM intraseasonal rainfall variability associated with the A-B periods produces a distinct spatial structure in the form of a quasi-east-west precipitation dipole with anomalies of one sign over northeast and southeast India and of opposite sign over western and central India [*Guhathakurta and Rajeevan*, 2008; *Rajeevan et al.*, 2010] (Figures 1 and S1 and S2 of the auxiliary material).[1] This spatial pattern is diminished (enhanced) in years marked by weak (strong) A-B periods. Thus, in principal, the inverse covariance (or lack-thereof) among precipitation records from respective hearts of the precipitation dipole can be used to assess

[1]Department of Earth Science, California State University Dominguez Hills, Carson, California, USA.
[2]Cooperative Institute for Research in Environmental Sciences, University of Colorado at Boulder, Boulder, Colorado, USA.
[3]Department of Earth Science, University of Southern California, Los Angeles, California, USA.
[4]Climate Risk Analysis, Hanover, Germany.
[5]Alfred Wegener Institute for Polar and Marine Research, Bremerhaven, Germany.
[6]Institute of Global Environmental Change, Xi'an Jiaotong University, Xi'an, China.
[7]Department of Geology and Geophysics, University of Minnesota, Minneapolis, Minnesota, USA.
[8]National Cave Research and Protection Organization, Raipur, India.

0094-8276/11/2011GL047713

[1]Auxiliary materials are available in the HTML. doi:10.1029/2011GL047713.

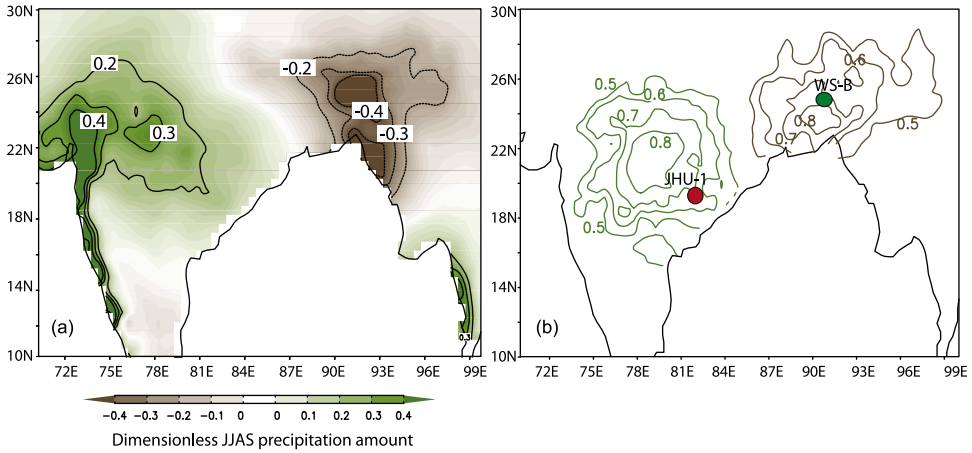

Figure 1. (a) First Empirical Orthogonal Function (EOF) of gridded Climate Research Unit (CRU) TS3.0 JJAS precipitation data from 1900-2006 (http://badc.nerc.ac.uk/data/cru/) shown as dimensionless precipitation units. The first EOF accounts for 22% of the overall rainfall variance, which is quite similar to the first EOF constructed from instrumental rainfall data consisting of 1476 stations from India, which explains 31% variance [*Guhathakurta and Rajeevan*, 2008]. (b) Correlation between JJAS precipitation from AD 1900 to 2006 from the CRU precipitation dataset for the grid point nearest to cave sites (JHU-1, green contours; WS-B, brown contours) grid cell. Figure 1 was made using the KNMI Climate Explorer (see http://climexp.knmi.nl).

the extent to which intraseasonal variability acts as a driver of monsoon variability. Here we present absolute dated, multicentennial-length speleothem-based precipitation reconstructions for central India (CI) and northeast India (NEI), which offer insight into the role of internal dynamics in generating ISM variability on centennial timescales during the last millennium.

2. Cave Locations and Climatology

[5] Monsoon precipitation and circulation patterns across the Indian subcontinent are radically different between active and break periods. Active period are characterized by a sequence of time-clustered convective systems, which bring heavy precipitation over central and western India, while during a typical break period, the monsoon trough (a NW-SE trending contiguous system of shallow thermal lows and moist convective lows across central India) shifts northward while convection is enhanced over the EIO resulting in drier conditions over much of the Indian subcontinent, and wetter conditions over the foothills of Himalayas and NEI [*Annamalai and Slingo*, 2001; *Guhathakurta and Rajeevan*, 2008; *Rajeevan et al.*, 2010] (Figures 1 and S1 and S2 of the auxiliary material). In this paper, we report $\delta^{18}O$ data from stalagmites collected from Jhumar Cave (18° 52′N, 81° 52′E; 600 masl) located near the town of Jagdalpur in CI, and Wah Shikar Cave (25° 15′N, 91° 52′E, 1290 masl) located ~30 km from the city of Shillong in NEI (Figure 1). The local annual precipitation variability at both sites is dominated by monsoon precipitation (July to September (JJAS); ~70–80%) (Tables S1 and S2 of the auxiliary material), which is strongly correlated with regional monsoon precipitation (Figure 1). In addition, the local to regional monsoon precipitation variability in both locations is strongly influenced by the frequency distribution of A-B periods (Figure S2 of the auxiliary material).

3. Materials, Chronology, and Instrumental Calibration

[6] We collected two actively growing stalagmites (JHU-1, ~91 mm and WS-B, ~93 mm) from Jhumar and Wah Shikar Caves in December 2008 and June 2009, respectively. Both stalagmite samples were removed from poorly ventilated chambers, located at considerable distances from the caves' entrance (~300 & 1000 m for Jhumar and Wah Shikar caves, respectively). Periodic measurements in Wah Shikar Cave and long-term (~2 yr) continuous measurements inside Jhumar Cave, indicate stable environmental conditions, characterized by high relative humidity (always in the excess of 95%), and nearly constant ambient temperatures (17.0 ± 0.3°C and 25.5 ± 0.5°C for Wah Shikar and Jhumar Caves, respectively) (Table S3 of the auxiliary material). Theoretical estimates of caves' ambient temperature, calculated from $\delta^{18}O$ measurements in dripwater and modern calcite from both chambers, are within the range of measured temperatures, suggesting that precipitation of calcite in both caves is occurring in isotopic equilibrium (Table S3 of the auxiliary material). Additionally, a high degree of replication between JHU-1 $\delta^{18}O$ profile during the period in which it overlaps with our previously reported $\delta^{18}O$ record from nearby (~20 km) Dandak Cave [*Sinha et al.*, 2007; *Berkelhammer et al.*, 2010] (AD 1075 to 1561, $n = 353$, $r = 0.62$ with 95% confidence interval [0.43; 0.74]) further supports this inference.

[7] The millennial-length JHU-1 $\delta^{18}O$ record (AD 1075 to 2008) contains 642 $\delta^{18}O$ measurements with an average temporal resolution of 1.45 years ($1\sigma = 0.73$ yr). The multicentennial-length (AD 1399 to 2007) speleothem $\delta^{18}O$

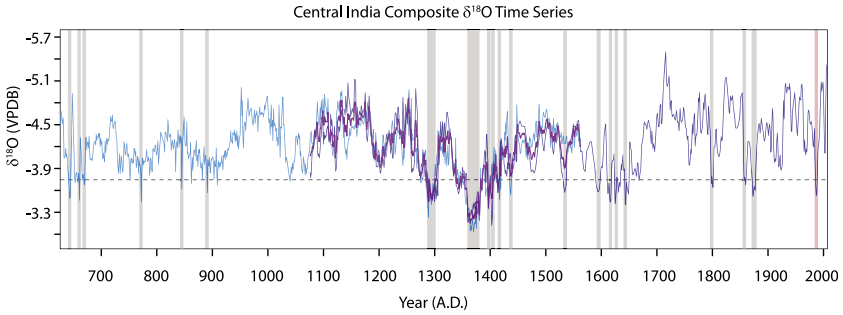

Figure 2. The $\delta^{18}O$ time series of JHU-1 (dark blue) and DAN-D (light blue) and JHU-1/DAN-D composite (purple) where up (down) on the y axis denotes moister (drier) condition, respectively. The $\delta^{18}O$ values >−3.8 ‰ (dashed line) mark periods of inferred drought [*Sinha et al.*, 2011]. The red bar denotes the most severe drought (year 1987) recorded during the instrumental period.

record (WS-B) from Wah Shikar Cave is established by 625 $\delta^{18}O$ measurements with an average temporal resolution of 0.97 years (1σ = 0.48 yr) (see the auxiliary material).

[8] The age model for WS-B stalagmite is developed from seven ^{230}Th dates, which are in correct stratigraphic order, with 2σ error ranging from 28 to 70 years (see the auxiliary material). Four additional ^{230}Th dates produced unreasonably high error (>100 years) and were subsequently discarded (Table S4 of the auxiliary material). The age model is developed by linearly interpolating between individual dates except for the segment between the bottom-two dates (Figure S3 of the auxiliary material) where we calculated the age at the bottom of the stalagmite by extrapolating the age-depth curve from two prior better-constrained dates. The differences between these two model curves produce an age difference of ~50 years at the beginning of the chronology (Figure S3 of the auxiliary material). The primary findings of this study are however, unaffected by the choice of age model used during this section of the time series (AD 1350 or 1399).

[9] The JHU-1 stalagmite is characterized by sub-mm length visible light-dark laminations, (Figure S7 of the auxiliary material) which we infer to be annual in nature (as described later). The JHU-1 chronology is established by counting growth laminae using both micrographs (50 x) and digitally enlarged (10 x) scanned images. Multiple counts along the growth axis by two researchers using digitally stitched micrographs and scanned images, respectively, suggest a total uncertainty of ~10 years at the bottom of the stalagmite. A suite of ^{230}Th dates were also obtained to test the annual nature of the laminations. While all ^{230}Th ages fall on or near the slope that describe the laminae-based age model (Figure S3 of the auxiliary material), we did not use ^{230}Th dates in the age model because of high detrital thorium in the JHU-1 stalagmite, which produced substantially large error in ^{230}Th dates (2σ > 200 years) (Table S4 of the auxiliary material). Our use of laminae-based chronology is however, well supported by the strong coherence between the JHU-1 and the absolute-dated DAN-D $\delta^{18}O$ profiles [*Sinha et al.*, 2007, 2011; *Berkelhammer et al.*, 2010] (r = 0.62 [0.43; 0.74]) (Figure 2). In addition, as described below, the JHU-1 $\delta^{18}O$ profile is significantly correlated with regional instrumental data, which further supports the robustness of laminae-based chronology.

[10] The JHU-1 $\delta^{18}O$ profile shows a significant inverse relationship with a regional (18°–27°N and 69°–88°E) JJAS precipitation time series (AD 1903–2005, n = 70, r = −0.46 [−0.59; −0.32]; Figure S4 of the auxiliary material), which reinforces the observation made in earlier studies that the $\delta^{18}O$ variations in speleothems and precipitation from this region primarily reflect changes in monsoon precipitation amount over CI [*Yadava and Ramesh*, 2005; *Sinha et al.*, 2007, 2011; *Berkelhammer et al.*, 2010; *Dayem et al.*, 2010]. A similar conclusion can also be drawn from a comparison of WS-B $\delta^{18}O$ time series with instrumental data from Shillong (AD 1867 to 2005), which reveals a moderately significant inverse correlation with JJAS precipitation (AD 1867–2005, n = 98, r = −0.31 [−0.43; −0.15]) (Figure S5 of the auxiliary material) and a moderately weak correlation with the surface mean annual temperatures (data available between AD 1903 and 1980, n = 49, r = 0.27 [0.12; 0.39]). The relatively weaker inverse correlation between $\delta^{18}O$ of precipitation and amount, however, imply that a portion of $\delta^{18}O$ variability in WS-B stalagmite (and thus, by extension, in precipitation over NEI) is produced by additional processes such as changes in the seasonal distribution of precipitation and/or vapor source and transport histories [*Breitenbach et al.*, 2010].

[11] The observed amount effect for NEI as recorded in WS-B stalagmite is not observable in $\delta^{18}O$ values in precipitation at the Global Network of Isotopes in Precipitation (GNIP) station in Shillong (years 1969 and 1976) or in an event-based study (snapshot $\delta^{18}O$ measurements of precipitation in years 2007 and 2008) [*Breitenbach et al.*, 2010]. Both data sets however, lack sufficient long-term observations, which preclude a definitive assessment of the presence or absence of amount effect. Notwithstanding, the intense convective nature of monsoon precipitation in NEI, and a presence of the statistically significant inverse correlation between the WS-B stalagmite $\delta^{18}O$ and instrumental precipitation data, lead us to call upon changes in monsoon precipitation amount as the primary source of $\delta^{18}O$ variations in precipitation at this site.

4. Results, Discussion, and Conclusions

[12] The JHU-1 stalagmite record from CI complements our previously reported millennial-length (AD 600 to 1500) reconstruction of monsoon precipitation variations from a

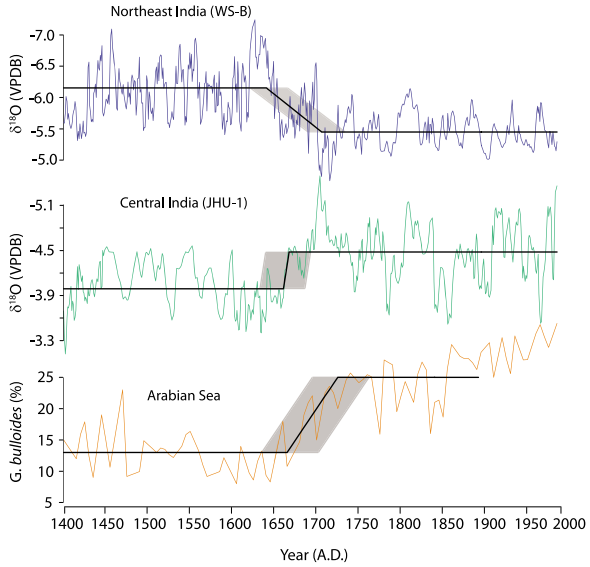

Figure 3. The $\delta^{18}O$ time series from JHU-1 (green), WS-B (blue) and Arabian Sea (orange) [*Anderson et al.*, 2002] from AD 1400 to 2000. The black line on each graph is the result of the ramp fitting procedure (Table S5 of the auxiliary material). The shaded region approximates the uncertainty in the timing of the change point based on a bootstrapping procedure [*Mudelsee*, 2010].

sub-annually resolved $\delta^{18}O$ record (DAN-D) from Dandak Cave, which is located ~20 km west of Jhumar Cave [*Sinha et al.*, 2007, 2011; *Berkelhammer et al.*, 2010]. By compositing the JHU-1 and DAN-D $\delta^{18}O$ records, we develop a continuous 1,400-year reconstruction of CI precipitation, which captures (within margin of dating error) major short-term droughts of the 20th century (e.g., AD 2002, 1985–87, 1964–1966, 1918–1920) (Figure S4 of the auxiliary material) as well as known historic failures of monsoon in India such as during AD 1876–78, 1861–63, and 1790–96 (Figure 2). In addition, the $\delta^{18}O$ record documents several instances of multi-year to decades-long intervals of reduced monsoon precipitation (Figure 2), particularly between the 13th and 17th centuries, which are corroborated by historical accounts of famines from India [e.g., *Sinha et al.*, 2007, 2011]. The $\delta^{18}O$ record also reveals lower frequency (centennial-scale) features, the most recent of which is a step-like transition (~0.5 ‰) between multiple centuries (AD 1400 to 1700) that were persistently drier than the 20th century norm, followed by a period (AD 1700 to 2007) where conditions remained in a more humid mean state (Figure 3).

[13] The WS-B $\delta^{18}O$ record is characterized by prominent multi-decadal scale $\delta^{18}O$ variability (1 to 2 ‰) and is anti-correlated with the JHU-1 $\delta^{18}O$ record on centennial timescales (AD 1399–2008, n = 390, r = −0.34 [−0.43; −0.13] (Figure 3). The most prominent aspect of this record is a step-like increase in $\delta^{18}O$ values during the late 17th century. Between AD 1400 and 1700, the mean $\delta^{18}O$ value (−6.2 ‰) is ~0.7‰ more negative than the mean $\delta^{18}O$ value between AD 1700 and 2008 (−5.5 ‰). We applied a change-point regression model using least-squares and brute-force search to the data to objectively estimate the timing of this shift (Table S5 of the auxiliary material) in both records [*Mudelsee*, 2010]. Uncertainty in the estimated change-points (timing and level) are derived from block bootstrap resampling (software RAMPFIT, 400 simulations) as described by *Mudelsee* [2010]. The timing of the late 17th century transition in CI and NEI records is indistinguishable within error, from each other as well as from a similar step in a marine record of variations in upwelling intensity from the Arabian Sea [*Anderson et al.*, 2002]. The latter captures variations in the strength of low level zonal wind across the Arabian Sea, and therefore, by extension, provides a measure of the ISM circulation strength.

[14] The JHU-1 and Arabian Sea records suggest a late 17th century shift towards enhanced monsoon precipitation and circulation, which has been previously documented in a number of proxy records of the Asian monsoon [e.g., *Sinha et al.*, 2011]. In contrast, the increase in the $\delta^{18}O$ values during (and since) the late 17th century in the WS-B stalagmite largely reflects a decrease in monsoon precipitation amount over NEI. The centennial scale spatial pattern of anti-phase monsoon precipitation variability over CI and NEI resemble the dipole structure associated with intraseasonal and interannual precipitation variability during the instrumental period [*Guhathakurta and Rajeevan*, 2008]. The similar spatial pattern (but on centennial timescale) inferred from our proxy records can be reconciled by calling upon low frequency changes in A-B periods as the dominant mode of ISM interannual variability over the last 600 years. We hypothesize that the interval from ~AD 1400 to 1700 was marked by a higher frequency and/or amplitude of break events, which on a year-to-year basis cumulatively generated centennial-scale episodes of negative (positive) precipitation anomalies over CI (NEI). We further hypothesize that the simultaneous shift to opposing precipitation regimes in both records during the late 17th century was caused by a change in the frequency characteristics of A-B periods. At the turn of the 17th century, the ISM dynamics shifted to a predominantly "active" state, generating precipitation anomalies of the opposite sign over CI and NEI. Our hypothesis does not diminish or exclude the role of "seasonally persisting" modes such as the Indo-Pacific SST anomalies in affecting monsoon precipitation on inter-annual or longer timescales [*Krishnamurthy and Shukla*, 2007]. Instead, we suggest that when viewed from a multi-century perspective, the dipole mode associated with intraseasonal oscillations, emerges as a more dominant source of ISM precipitation variability as opposed to continent-wide changes in monsoon precipitation.

[15] The inferred multicentennial length episodes of "break-dominated" and "active-dominated" states imply that the external boundary conditions predispose ISM to reside in these modes. By the same token, we suggest that changes in some aspect of the external boundary conditions, such as land-sea surface thermal contrast may have triggered the late 17th century shift in ISM behavior through their impact on the frequency characteristics of A-B periods. We have previously suggested that a northward shift in the mean latitude of the intertropical convergence zone (ITCZ) accompanied by stronger low-level monsoon westerlies is a plausible mechanism to account for the strengthening of monsoon across the 17th century [*Sinha et al.*, 2011]. The results presented here further suggest that the planetary-scale ITCZ changes directly influenced ISM precipitation by modulating the frequency distribution of A-B periods. This inference finds support in observational and modeling studies,

which suggest that positive feedbacks between monsoon westerlies and the upwelling intensity in the EIO modulate deep convection over the EIO, which in turn, affects the frequency and amplitude of A-B periods [*Krishnan et al.*, 2006]. Additionally, the ISM regime change across the 17th century appears to have occurred in close temporal relationship with an inferred decrease in the zonal SST gradient across the equatorial Pacific [*Conroy et al.*, 2010], suggesting that changes in the Indo-Pacific tropical hydrology and/or El Niño/Southern Oscillation (ENSO) properties (Figure S6 of the auxiliary material) may also be important. Some empirical evidence indeed exists to suggest that warm (cold) SST anomalies in the tropical Pacific modify the PDF towards more break (active) regimes but the brevity of instrumental record hampers a definitive assessment of such linkages [*Webster et al.*, 1998; *Annamalai et al.*, 1999].

[16] The paleoclimate data presented in this paper suggest that the ISM can persist in a predominantly active or break mode for centuries. The switch between these states occurs rapidly (within decades,) implying the system can respond with non-linear or threshold type behavior to forcings [*Levermann et al.*, 2009; *Schewe et al.*, 2011; *Sinha et al.*, 2011]. The latter observation may prove significant in considering how the ISM may respond to a warming global climate. For example, an increased occurrence of break spells, delayed monsoon onset, and weaker cross-equatorial monsoonal winds appear as robust features in simulations with a high resolution nested climate model in response to projected greenhouse forcing in the 21st century [*Ashfaq et al.*, 2009], suggesting that ISM could potentially experience a mode-switch comparable to the one we document in our proxy records.

[17] **Acknowledgments.** We thank M. Rajeevan and the Indian Meteorological Department for providing Indian monsoon instrumental data; A. Arceo, H. Ahmadzai, and M. Rincon for laboratory analysis; B. Khapran-Daly, T. Mawlong, and R. Berkelhammer for the field support; A. Levermann for helpful comments on our manuscript; and the staff at the Kanger Valley National Park (Chhattisgarh), India for providing access to Jhumar Cave. This work was supported by the National Science Foundation grant to A.S. (ATM: 0823554).

[18] The Editor wishes to acknowledge Anders Levermann and two anonymous reviewers for the assistance evaluating this manuscript.

References

Anderson, D. M., J. T. Overpeck, and A. K. Gupta (2002), Increase in the Asian Southwest Monsoon during the past four centuries, *Science*, *297*, 596–599, doi:10.1126/science.1072881.

Annamalai, H., and J. M. Slingo (2001), Active/break cycles diagnosis of the intraseasonal variability of the Asian Summer Monsoon, *Clim. Dyn.*, *18*, 85–102, doi:10.1007/s003820100161.

Annamalai, H., J. M. Slingo, K. R. Sperber, and K. Hodges (1999), The mean evolution and variability of the Asian summer monsoon: Comparison of ECMWF and NCEP–NCAR Reanalyses, *Mon. Weather Rev.*, *127*, 1157–1186, doi:10.1175/1520-0493(1999)127<1157:TMEAVO>2.0.CO;2.

Ashfaq, M., Y. Shi, W. Tung, R. J. Trapp, X. Gao, J. S. Pal, and N. S. Diffenbaugh (2009), Suppression of South Asian summer monsoon precipitation in the 21st century, *Geophys. Res. Lett.*, *36*, L01704, doi:10.1029/2008GL036500.

Berkelhammer, M., A. Sinha, M. Mudelsee, and K. G. Cannariato (2010), Persistent multidecadal power in the Indian Summer Monsoon, *Earth Planet. Sci. Lett.*, *290*, 166–172, doi:10.1016/j.epsl.2009.12.017.

Breitenbach, S., et al. (2010), Strong influence of water vapor source dynamics on stable isotopes in precipitation observed in Southern Meghalaya, NE India, *Earth Planet. Sci. Lett.*, *292*, 212–220, doi:10.1016/j.epsl.2010.01.038.

Charney, J. G., and J. Shukla (1981), *Predictability of Monsoons: Monsoon Dynamics*, Cambridge Univ. Press, New York.

Conroy, J. L., J. T. Overpeck, and J. E. Cole (2010), El Niño/Southern Oscillation and changes in the zonal gradient of tropical Pacific sea surface temperature over the last 1.2 ka, *PAGES News*, *18*, 32–34.

Dayem, K., P. Molnar, D. Battisti, and G. Roe (2010), Lessons learned from oxygen isotopes in modern precipitation applied to interpretation of speleothem records of paleoclimate from eastern Asia, *Earth Planet. Sci. Lett.*, *295*, 219–230, doi:10.1016/j.epsl.2010.04.003.

Goswami, B. N., and R. S. Ajaya Mohan (2001), Intraseasonal oscillations and interannual variability of the Indian summer monsoon, *J. Clim.*, *14*, 1180–1198, doi:10.1175/1520-0442(2001)014<1180:IOAIVO>2.0.CO;2.

Goswami, B. N., G. Wu, and T. Yasunari (2006), The annual cycle, intraseasonal oscillations, and roadblock to seasonal predictability of the Asian Summer Monsoon, *J. Clim.*, *19*, 5078–5099, doi:10.1175/JCLI3901.1.

Guhathakurta, P., and M. Rajeevan (2008), Trends in the rainfall pattern over India, *Int. J. Climatol.*, *28*, 1453–1469, doi:10.1002/joc.1640.

Krishnamurthy, V., and J. Shukla (2000), Intraseasonal and interannual variability of rainfall over India, *J. Clim.*, *13*, 4366–4377, doi:10.1175/1520-0442(2000)013<0001:IAIVOR>2.0.CO;2.

Krishnamurthy, V., and J. Shukla (2007), Intraseasonal and seasonally persisting patterns of Indian monsoon rainfall, *J. Clim.*, *20*, 3–20, doi:10.1175/JCLI3981.1.

Krishnan, R., K. V. Ramesh, B. K. Samala, G. Meyers, J. M. Slingo, and M. J. Fennessy (2006), Indian Ocean monsoon coupled interactions and impending monsoon droughts, *Geophys. Res. Lett.*, *33*, L08711, doi:10.1029/2006GL025811.

Levermann, A., J. Schewe, V. Petoukhov, and H. Held (2009), Basic mechanism for abrupt monsoon transitions, *Proc. Natl. Acad. Sci. U. S. A.*, *106*, 572–577.

Mudelsee, M. (2010), *Climate Time Series Analysis: Classical Statistical and Bootstrap Methods*, Springer, New York.

Palmer, T. N. (1994), Chaos and predictability in forecasting the monsoons, *Proc. Indian Natl. Sci. Acad.*, *60*, 57–66.

Rajeevan, M., S. Gadgil, and J. Bhate (2010), Active and break spells of the Indian summer monsoon, *J. Earth Syst. Sci.*, *119*, 229–247, doi:10.1007/s12040-010-0019-4.

Schewe, J., A. Levermann, and H. Cheng (2011), A critical humidity threshold for monsoon transitions, *Clim. Past Discuss.*, *7*, 1737–1765, doi:10.5194/cpd-7-1737-2011.

Sinha, A., et al. (2007), A 900 year (600 to 1500 AD) record of the Indian Summer Monsoon precipitation from the core monsoon zone of India, *Geophys. Res. Lett.*, *34*, L16707, doi:10.1029/2007GL030431.

Sinha, A., et al. (2011), A global context for megadroughts in monsoon Asia during the past millennium, *Quat. Sci. Rev.*, *30*, 47–62, doi:10.1016/j.quascirev.2010.10.005.

Webster, P. J., et al. (1998), Monsoons: Processes, predictability, and the prospects for prediction, *J. Geophys. Res.*, *103*, 14,451–14,510, doi:10.1029/97JC02719.

Yadava, M. G., and R. Ramesh (2005), Monsoon reconstruction from radiocarbon dated tropical Indian speleothems, *Holocene*, *15*, 48–59, doi:10.1191/0959683605h1783rp.

M. Berkelhammer, Cooperative Institute for Research in Environmental Sciences, University of Colorado at Boulder, Boulder, CO 80309, USA.

J. Biswas, National Cave Research and Protection Organization, 3/40 Civil Lines, Rajatalab, Raipur, 492001 CG, India.

H. Cheng, Institute of Global Environmental Change, Xi'an Jiaotong University, Xi'an, Shaanxi 710049, China.

M. Mudelsee, Climate Risk Analysis, Schneiderberg 26, Hanover D-30167, Germany.

A. Sinha, Department of Earth Science, California State University Dominguez Hills, Carson, CA 90747, USA.

L. Stott, Department of Earth Science, University of Southern California, Los Angeles, CA 90747, USA.